


ORIGINAL ARTICLE

Investigation of pelvic symmetry: A systematic analysis using computer aided design software

Qiubao Zheng^{1,2}  | Kangshuai Xu³ | Xiaorui Zhan⁴ | Fuming Huang⁵ | Liping Wang⁶ | Sheqiang Chen¹ | Jiacheng Li¹ | Cheng Yang¹ | Yuhui Chen¹ | Shicai Fan¹

¹The Third Affiliated Hospital of Southern Medical University, Guangzhou, China

²Panyu Central Hospital, Guangzhou, China

³Department of Orthopedics, Jinhua Municipal Central Hospital, Jinhua, China

⁴Huizhou First People's Hospital, Huizhou, China

⁵Maoming People's Hospital, Maoming, China

⁶University of South Australia, Adelaide, South Australia, Australia

Correspondence

Cheng Yang, Yuhui Chen, and Shicai Fan, The Third Affiliated Hospital of Southern Medical University, Guangzhou, CN 510663, China.

Email: yangchengsmu@163.com, ah1990726@163.com, and 553924952@qq.com

Funding information

Clinical Research Startup Program of Southern Medical University by High-level University Construction Funding of Guangdong Provincial Department of Education, Grant/Award Number: LC2016ZD032; National Natural Science Foundation of China, Grant/Award Numbers: 81772428, 82072411; Special Program of Guangdong Frontier and Key Technological Innovation, Grant/Award Number: 2015B010125006; Innovation fund cultivation project of National Clinical Research Center for Orthopedics Sports Medicine & Rehabilitation, Grant/Award Number: 2021-NCRC-CXJJ-PY-06

Abstract

Objectives: This study aimed to investigate the symmetry of the Chinese pelvis.

Methods: Computed tomography scan images of each of 50 Chinese pelvises were converted to 3D models and the left sides of the pelvises were reflected on Mimics software. Then, the reflected left side model was aligned with the right side using the closest point algorithm function of Geomagic software to perform symmetry analysis. The volume and surface area of either side of the pelvises were also calculated. The mean standard deviation (SD), the mean percentage of permissible deviations within the ± 2 mm range, the percentage differences in volume and surface area were measured to compare pelvic symmetry. In addition, the distribution of pelvic bilateral symmetry associated with both age and sex were compared.

Results: The mean SD was 1.15 ± 0.16 mm and the mean percentage of permissible deviations was $90.82\% \pm 4.67\%$. The deviation color maps showed that the specific areas of asymmetry were primarily localized to major muscle or ligament attachment sites and the sacroiliac joint surfaces. There was no significant difference between the bilateral sides of the pelvis in either volume or surface area. Additionally, no difference in any indexes was exhibited in relation to sex and age distribution.

Abbreviations: CAD, computer aided design; CT, computed tomography; DCMs, deviation color maps; SD, standard deviation.

Qiubao Zheng, Kangshuai Xu, Xiaorui Zhan, and Fuming Huang contributed equally to this work.

This is an open access article under the terms of the Creative Commons Attribution-NonCommercial-NoDerivs License, which permits use and distribution in any medium, provided the original work is properly cited, the use is non-commercial and no modifications or adaptations are made.

© 2022 The Authors. *Health Care Science* published by John Wiley & Sons Ltd on behalf of Tsinghua University Press.

Conclusion: Our results demonstrated that the pelvis has high bilateral symmetry, which confirmed the potential of using contralateral pelvic models to create fully patient-specific and custom-made pelvic implants applicable for the treatment of fracture and bony destruction.

KEYWORDS

3D models, deviation analysis, pelvis, surgical planning, symmetry

1 | INTRODUCTION

The pelvis is the atlas of human weight bearing within one of the most complex bony structures in the human skeletal system. Physical disability frequently results after suffering a pelvic injury such as a fracture or bony destruction caused by tumors or infection [1–3]. However, current implants cannot provide ideal anatomical matches for reconstruction of the pelvis due to its irregular surface and construction [4]. Technical improvements in 3D printing have allowed the development of personal specific designs of implants over past decades [5]. Nevertheless, the disrupted hemi-pelvis as a result of trauma or destruction always results in the absence of reference data for 3D printing applications [6]. Although recent publications claimed positive effects in the treatment of pelvic disruption by using 3D-printed implants based on contralateral pelvic models, the symmetry of the bilateral pelvis has not been confirmed in detail in different populations [6, 7].

In this study, the bilateral symmetry of the Chinese pelvis was analyzed using computer aided design (CAD) software. Simultaneously, the distribution of pelvic bilateral symmetry associated with both age and sex was also compared.

2 | MATERIALS AND METHODS

2.1 | Patients and scan images

Candidates were chosen from the computed tomography (CT) scan image database of the imaging department in the Third Affiliated Hospital of Southern Medical University. The images were stored in a DICOM file format. A total of 50 patients were identified from the database and involved in our study (28 males, 22 females, age range from 14 to 70 years with a mean age of 38.18 ± 16.52 years). There were 22 persons aged <30 years, 18 aged 30–60 years and 10 aged >60 years. None of them complained of lower limb motion disabilities or had undergone any surgical treatments involving the pelvis. The typical parameter was 512×512

pixels per slice and the mean slice thickness was 0.75 mm (range 0.5–1 mm). The scans were previously obtained for other clinical purposes such as health examination and were retrospectively reviewed for this study, thus the scanner parameters were not standardized across participants. This retrospective study conforms to the provisions of the Declaration of Helsinki (as revised in Brazil in 2013) and was approved by the Ethics Committee of The Third Affiliated Hospital of Southern Medical University. Patients previously provided consent to participate in research.

2.2 | Construction of 3D models

Reconstructions and analysis were all performed by a senior engineer. All the 3D models were constructed, modified, and analyzed through the same standardization process.

The DICOM files were imported into Materialize Mimics (Materialize, Leuven, Belgium, version 21), using a lossless compression technique, to create the 3D digitized models. Materialize Mimics is medical image processing software extensively used in neurology, cardiology, and orthopedics [8–10]. First, a “bone mask” was created to isolate the pixels of bony tissue, then the segmenting tool in Mimics was used to construct the reflected left side and the right side of pelvic models, followed by “edit mask” to eliminate the pixels of surrounding soft tissue and noise, and to remove the pixels of the spine, femurs, and sacrum, then “region grow” to create two isolated masks, which represented one for each side of the pelvis, “calculate part” to construct 3D models, and “mirror” to reflect the left side model across the sagittal plane (defined by the YZ plane in the image coordinate system). Finally, the reflected left side and the right side of the pelvic models were exported as separate STL files (Figure 1).

2.3 | The 3D deviation analysis

To maximally reconstruct the anatomy and 3D geometry of the pelvis, the two STL files were imported into

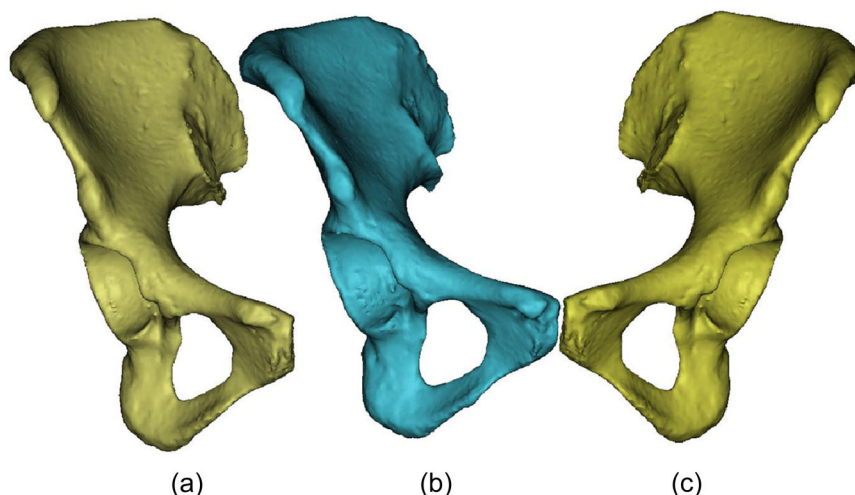


FIGURE 1 A 3D pelvis model created in Mimics by reflection of the left side of the pelvis. (a) The reflected left side model. (b) The right side model. (c) The left side model.

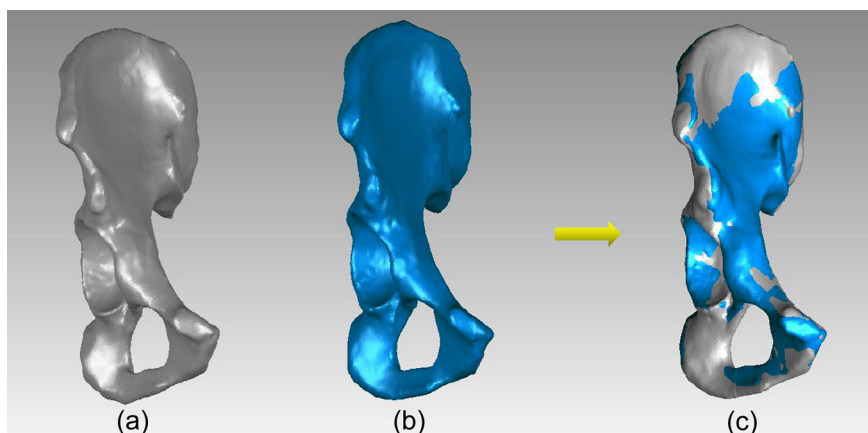


FIGURE 2 Alignment of two models in Geomagic. (a) The reflected right side is shown in gray. (b) The right side is shown in blue. (c) Aligning the reflected left side and the right side of the pelvis using the best-fit alignment function.

Geomagic Studio 2013 (Geomagic), reverse engineering software widely used in industrial design and the 3D printing industry [11–13]. After using “Remash” to precisely recreate the point cloud and “Remove Spikes” to detect and flatten the single-point spikes on the polygon, the two 3D models were exported as separate WRP files.

The WRP files were imported into Geomagic Qualify 2013, which is a standard tool used in technical comparisons of 3D models [14, 15], to compare the symmetry of bilateral sides of the pelvis. The two objects were aligned by using the “best-fit alignment” function (Figure 2). The “best-fit alignment” function can minimize the distance between two objects through an iterative closest point algorithm. In this analysis, the technician defined the right side of the pelvic models as the reference object, the reflected left side as the test

object. A comparative report can be generated automatically after 3D comparison, including the standard deviation (SD) of values and the percentage of permissible deviations. The SD reflects the distance of each point between two three-dimensional planes, which comprehensively consider the positive and negative deviations between two objects to avoid a situation in which they offset each other. The percentage of permissible deviation indicates that the deviations are within the preset threshold range, which is sufficient to prove the symmetry hypothesis. They were used for quantitative and qualitative analysis of the difference between surfaces.

The comparative report also provides deviation color maps (DCMs), which are a visual and quantitative representation of deviations between the left and right sides of the pelvis. To quantitatively analyze and compare

the results, a threshold of ± 2 mm deviation was specified as the permissible deviation (the green regions of the DCMs) for symmetry, based on results in the literature, which concluded that a reduction within 2 mm was considered acceptable in terms of preventing osteoarthritis in the hip joints [1, 7, 16]. Additionally, the impermissible deviations (red/blue regions of the DCMs) for asymmetry were set outside the range of ± 2 mm.

2.4 | Volume and surface area

The volume and surface area of each side of the pelvises was also obtained using Geomagic Qualify and the corresponding variations between the left and right sides were calculated. As the pelvis is constructed of cortical bone in the outer layer and cancellous bone on the inside, we calculated the volume of the material of a part rather than the volume contained within the outline of the part by using Geomagic. It was necessary to fill the pelvic volume to create a solid bone model so that we could make a fair comparison and eliminate the influences of the depth of the cortical bone layer.

2.5 | Statistical analysis

Statistical analysis was conducted with SPSS 22.0 (SPSS Inc). Students' *t*-test was used to evaluate the differences

between the sexes in each distribution and one-way analysis of variance was used to evaluate the differences within each distribution of age. The differences of the volume and the surface area between corresponding pelvis sides was evaluated by paired *t*-tests. Level of significance was set at $p < 0.05$.

3 | RESULTS

In our results, the mean SD was 1.15 ± 0.16 mm and the mean percentage of permissible deviations was $90.82\% \pm 4.67\%$. Simultaneously, the percentage difference in volume and surface area between the right and left side of the pelvic models was $0.39\% \pm 2.48\%$ and $0.30\% \pm 1.78\%$, respectively. No significant difference was observed between the sides of the pelvis in either volume or surface area (Table 1). Additionally, no difference in any indexes was exhibited with regard to sex and age distribution (Table 1). These results suggesting that the bilateral pelvises were symmetric.

The green areas (permissible deviations) of the DCMs representing the deviations between the right and left side surfaces were minor (< 2 mm), whereas the red/blue areas (representing impermissible deviations) were large (> 2 mm) (Figures 3 and 4). The mean rate of impermissible deviations (specific areas of pelvises) was $9.18\% \pm 4.67\%$ in overall deviations, and their probability was quantified as

TABLE 1 The overall deviation and the differences within each distribution of sex and age on symmetry

Items	Mean variable			
	Standard deviation (mm)	Percentage of permissible deviations (%)	Percentage differences in volume (%)	Percentage differences in surface area (%)
<i>Sex</i>				
M	1.12 ± 0.17	91.98 ± 3.51	0.15 ± 2.76	0.15 ± 1.34
F	1.18 ± 0.15	89.79 ± 5.13	0.69 ± 2.10	0.48 ± 2.25
<i>p</i>	0.20	0.08	0.46	0.52
<i>Age (years)</i>				
<30	1.11 ± 0.16	91.01 ± 5.15	0.80 ± 2.52	0.68 ± 2.40
30–60	1.17 ± 0.18	90.65 ± 4.95	0.01 ± 2.83	0.18 ± 1.04
>60	1.19 ± 0.11	90.70 ± 3.04	0.18 ± 1.71	0.33 ± 1.03
<i>p</i>	0.27	0.97	0.58	0.32
<i>Overall</i>				
	1.15 ± 0.16	90.82 ± 4.67	0.39 ± 2.48	0.30 ± 1.78
<i>p</i>	-	-	0.27	0.24

Note: Overall refers to the comparisons data of bilateral pelvic for all individuals regardless of sex and age.

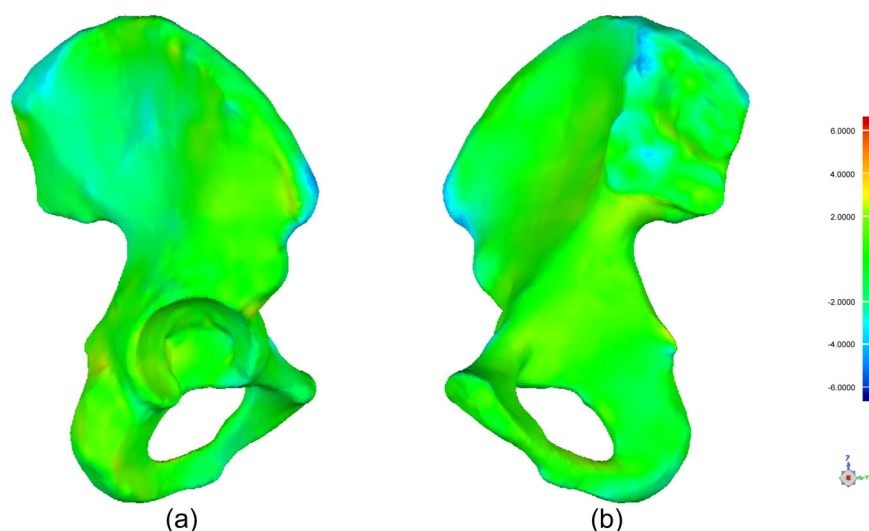


FIGURE 3 DCMs produced by 3D deviation analysis in Geomagic. (a) Posterior view. (b) Anterior view. DCMs, deviation color maps.

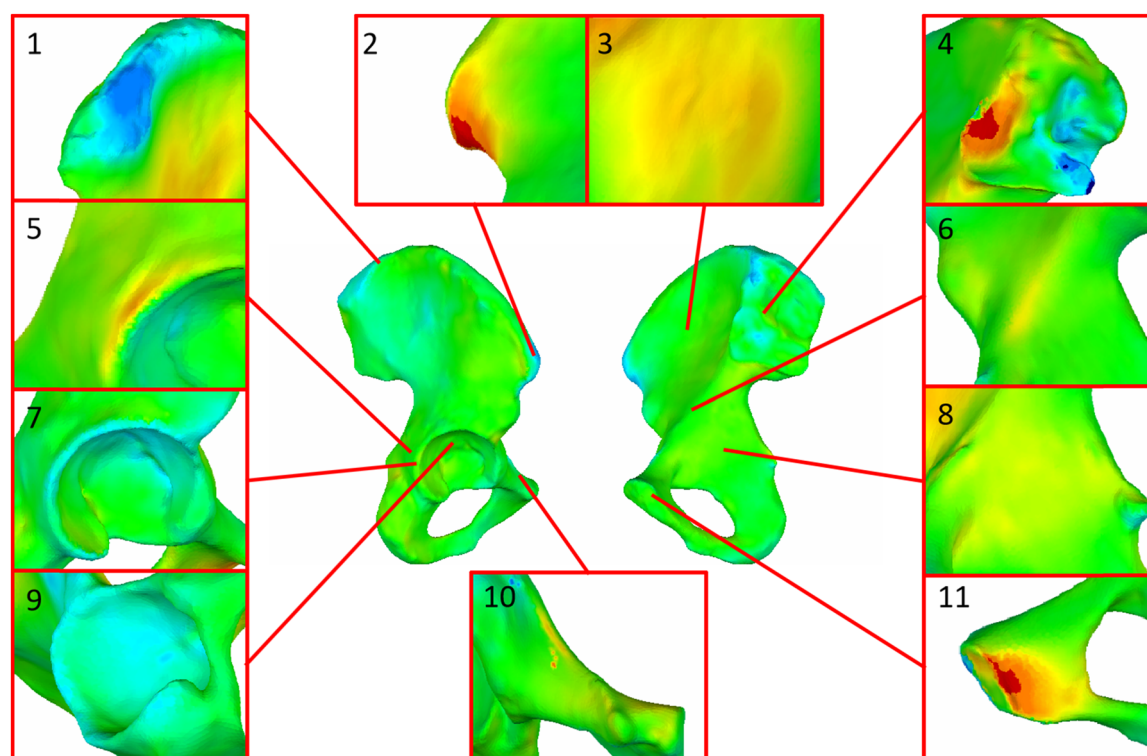


FIGURE 4 The DCMs intuitively showed the specific areas of pelvises with impermissible deviations. They include: (1) The iliac crest, (2) The iliac spines, (3) The iliac fossa, (4) The sacroiliac joint surface, (5) The posterior wall of the acetabulum, (6) The arcuate line, (7) The acetabular labrum, (8) The quadrilateral area, (9) The acetabular fossa, (10) The superior pubic ramus, (11) The surrounding structure of pubic symphysis. DCMs, deviation color maps.

shown in Table 2. The majority of impermissible deviations were primarily localized to major muscle or ligament attachment sites, including the iliac crest (16%), the iliac spines (24%), the surrounding structure of the pubic symphysis (14%), and the sacroiliac joint surface (34%). In contrast,

only a few of them were localized to the other areas of the iliac fossa (2%), the quadrilateral area (2%), the arcuate line (4%), the superior pubic ramus (4%), the posterior wall of the acetabulum (2%), the acetabular labrum (2%), and the acetabular fossa (4%).

TABLE 2 The probability of impermissible deviations of specific areas of the pelvis

Probability (%)											
Items	Surrounding structure of the pubic symphysis			Sacroiliac joint surface	Iliac fossa	Quadrilateral area	Arcuate line	Superior pubic ramus	Posterior wall of acetabulum	Acetabular labrum	Acetabular fossa
	Iliac crest	Iliac spines									
Sex											
M	14.3	21.4	14.3	35.7	0.0	3.6	3.6	3.6	3.6	0.0	3.6
F	18.2	27.3	13.6	31.8	4.5	0.0	4.5	4.5	0.0	4.5	4.5
Age (years)											
<30	13.6	22.7	13.6	36.4	4.5	4.5	4.5	4.5	0.0	0.0	4.5
30–60	16.7	22.2	11.1	33.3	0.0	0.0	0.0	5.6	5.6	0.0	0.0
>60	20.0	30.0	20.0	30.0	0.0	0.0	10.0	0.0	0.0	10.0	10.0
Overall											
16.0	24.0	14.0	34.0	2.0	2.0	4.0	4.0	2.0	2.0	2.0	4.0

Note: The iliac spines were referred to the anterior superior iliac spine, the anterior inferior iliac spine, the posterior superior iliac spine, and the posterior inferior iliac spine, and the surrounding structure of pubic symphysis includes the symphyseal surface, the pubic crest and the pubic tubercle in this study.

4 | DISCUSSION

The individual specific design of implants is still lacking in the treatment of fracture and bony destruction of the pelvis [1]. Otherwise, inappropriate implants may result in biomechanical differences between the reconstructed and intact sides or in unsatisfactory reduction [6]. The development of patient-specific and custom-made 3D implant models should help to meet the clinical requirements [4]. Studying the overall shape of the pelvis and confirming pelvic symmetry would aid surgeons in developing quicker and better treatment proposals and building fully-intact patient-specific and custom-made implants using contralateral pelvic models, which would help to reduce surgical operation time, bleeding volume and operation-related risks [17-21]. Once these implants are well placed, surgeons reasonably believe that they are of good quality for fracture reconstruction and bone defect restoration.

Previous studies focused on the parameters of anatomical landmarks, major pelvic diameter lines, or pre-shaped implants that may be indicative of pelvic symmetry [22-24]. Boulay et al. used 71 variables (based on pelvic anatomical landmarks) to quantify left-right symmetry of 12 pelvic specimens and concluded that 56 of the variables were symmetric [22]. Taller et al. compared the lengths of bilateral arcuate lines at the pelvic inlet among 50 pelvises and found that 86% had a high anatomical similarity while 14% had a significant difference [23]. Osterhoff et al. confirmed that the periacetabular surface of the pelvis is symmetric by comparing the differences between either side of the pelvis and a virtual reference implant [24]. Despite the significance of these studies, they failed to capture the entire 3D geometric shape of the pelvis. Ead et al. tried to confirm pelvic symmetry by using CAD software to examine the entire 3D geometric shape of 14 test subjects and their results also confirmed that the pelvis is symmetric [7]. However, because there were so few test subjects and lack of detailed analysis of sex and age distribution, which may influence pelvic symmetry, there is no doubt that further research is needed to study the symmetry.

To avoid these limitations, we further evaluated the pelvic symmetry of 50 pelvises using CAD software and analyzed whether symmetry was confirmed over sex and age distribution. CT scan images of each of the 50 subjects involved in the study were converted to 3D models and the left sides of the pelvises were reflected on Mimics (Figure 1). Then, the reflected left side model was aligned with the right side using a closest point algorithm function of Geomagic (Figure 2) to conduct symmetry analysis. To compare pelvic symmetry, we primarily

analyzed the date of the mean SD and the mean percentage of permissible deviations produced by DCMs (Table 1). It is important to note that the mean SD was small (1.15 ± 0.16 mm) and the mean percentage of permissible deviations was large ($90.82\% \pm 4.67\%$), suggesting that the bilateral hemi-pelvises were, indeed, symmetric. Meanwhile, the volume and surface area of either side of the pelvises were also obtained from Geomagic and their percentage differences were calculated (Table 1). These differences were small and showed no significant differences ($p = 0.27$ and $p = 0.24$, respectively), which further supported the conclusion of the symmetry. These results were also consistent with previous studies [7, 24].

In addition, whether bilateral symmetry could be confirmed across sex and age distribution were also analyzed and the results showed that there was no significant difference (Table 1), which indicated that age and sex may be irrelevant to bilateral symmetry. Although the CT scan images of older people showed lower bone density and it was more difficult to completely reconstruct the entire 3D geometry of the pelvis, which may lead to an increase in error, there was no significant difference related to sex and age distribution in our study.

From the DCMs (Figure 4) we could intuitively identify some asymmetric areas of pelvises with impermissible deviations and their probability is shown in Table 2. The majority of them were primarily localized to major muscle or ligament attachment sites, which might cause difficulties in manual segmentation processing. Particularly, the largest differences in the sacroiliac joint surface (34%) might be due to its irregular surface. However, because these regions were not common positions for internal fixation, relatively large differences between the right and left side of the pelvis would not affect the viability of using contralateral pelvic models. In contrast, only a few (range 2%–4%) of impermissible deviations were localized to the areas of common positions for internal fixation. These differences were also mentioned in previous studies [7, 24]. In other words, these impermissible deviations did not significantly affect the clinical application of pelvic symmetry and as a result we were less concerned about their effect in these contexts.

Although the present study was meaningful, there were a few limitations to note. Because the considerable noise of some CT scan images caused by interference from muscle or ligaments caused difficulties in manual segmentation processing, the large deviations found in some areas of the pelvis may be a result of this or simply due to individual differences of the bilateral hemi-pelvis. Even for the most experienced surgeons or technicians,

reducing the error of manual segmentation and reconstructing the entire 3D geometry of the pelvis is very difficult. However, measures can be taken to reduce these errors, including using CT scans with smaller slice thicknesses to accurately scan the anatomical structure of the pelvis and being more familiar with the anatomy of the pelvis. On the other hand, this symmetry theory is only applicable for unilaterally-fractured pelvises or bone defects so that bilaterally-fractured pelvises or bone defects cannot be reconstructed using this method unless the fractures or bone defects on each side do not occur in the same location or there are available CT scan images of the healthy intact pelvis before disease onset; however, this approach has not yet been investigated [25]. Likewise, it does not reliable for surgical reduction of pelvic and acetabular fractures in patients with congenital dysplasia such as DDH. Taking all these into account, the contralateral pelvic models are still a feasible and effective way to achieve the design of patient-specific and custom-made pelvic implants for the treatment of fracture and bony destruction.

5 | CONCLUSION

This investigation using CAD software avoided some limitations of previous studies and filled an important research gap in the literature of pelvic symmetry. The bilateral hemi-pelvises showed a high degree of symmetry obtained from extrapolation of the data, including the mean SD, the mean percentage of permissible deviations, and the percentage differences in volume and surface area. Additionally, no difference in any indexes was exhibited in relation to sex and age distribution. The specific areas of asymmetry were primarily localized to major muscle or ligament attachment sites and the sacroiliac joint surfaces. Nevertheless, because these regions were not common positions for internal fixation, they were clinically insignificant in the context of using the contralateral pelvic model for surgical planning. As a result, it would be feasible and effective to apply the concept of pelvic symmetry to create fully patient-specific and custom-made pelvic implants by using contralateral pelvic models for the treatment of fracture and bony destruction.

AUTHOR CONTRIBUTIONS

Qiubao Zheng: Data curation (lead); methodology (lead); project administration (lead); software (lead); writing – original draft (lead); writing – review and editing (equal). **Kangshuai Xu:** Data curation (equal); Software (equal); writing – original draft (equal). **Xiaorui Zhan:** Data curation (equal); Software (equal); writing – original draft

(equal). **Fuming Huang**: Data curation (equal); methodology (equal). **Liping Wang**: Data curation (equal). **Sheqiang Chen**: Data curation (equal); software (equal). **Jiacheng Li**: Data curation (equal); software (equal). **Cheng Yang**: Supervision (equal); writing – review and editing (equal). **Yuhui Chen**: Writing – original draft (equal); writing – review and editing (equal). **Shicai Fan**: Project administration (lead); writing – review and editing (lead).

ACKNOWLEDGMENTS

We thank International Science Editing (<http://www.internationalscienceediting.com>) for editing this manuscript. This study was funded by Clinical Research Startup Program of Southern Medical University by High-level University Construction Funding of Guangdong Provincial Department of Education, grand/award number: LC2016ZD032. National Natural Science Foundation of China, grand/award number: 81772428 and grand/award number: 82072411. Special Program of Guangdong Frontier and Key Technological Innovation, grand/award number: 2015B010125006. Innovation fund cultivation project of National Clinical Research Center for Orthopedics Sports Medicine & Rehabilitation (2021-NCRC-CXJJ-PY-06).

CONFLICT OF INTEREST

The author declares no conflict of interest.

DATA AVAILABILITY STATEMENT

The data of our article is availability.

ETHICS STATEMENT

Not applicable.

INFORMED CONSENT

Not applicable.

ORCID

Qiubao Zheng  <http://orcid.org/0000-0002-4628-5828>

REFERENCES

1. Boudissa M, Courvoisier A, Chabanas M, Tonetti J. Computer assisted surgery in preoperative planning of acetabular fracture surgery: state of the art. *Expert Rev Med Devices*. 2018;15:81–9. <https://doi.org/10.1080/17434440.2017.1413347>
2. Danışman M, Mermerkaya MU, Bekmez Ş, Ayvaz M, Atilla B, Tokgözoğlu AM. Reconstruction of periacetabular tumours with saddle prosthesis or custom-made prosthesis, functional results and complications. *Hip Int*. 2016;26:e14–8. <https://doi.org/10.5301/hipint.5000306>
3. Wei R, Guo W, Ji T, Zhang Y, Liang H. One-step reconstruction with a 3D-printed, custom-made prosthesis after total en bloc sacrectomy: a technical note. *Eur Spine J*. 2017;26:1902–9. <https://doi.org/10.1007/s00586-016-4871-z>
4. Nieminen J, Pakarinen TK, Laitinen M. Orthopaedic reconstruction of complex pelvic bone defects. Evaluation of various treatment methods. *Scand J Surg*. 2013;102:36–41. <https://doi.org/10.1177/145749691310200108>
5. Chen X, Xu L, Wang Y, Hao Y, Wang L. Image-guided installation of 3D-printed patient-specific implant and its application in pelvic tumor resection and reconstruction surgery. *Comput Methods Programs Biomed*. 2016;125:66–78. <https://doi.org/10.1016/j.cmpb.2015.10.020>
6. Chana Rodriguez F, Perez Mananes R, Narbona Carceles FJ, Gil Martinez P. 3D printing utility for surgical treatment of acetabular fractures. *Rev Esp Cir Ortop Traumatol*. 2018;62(4):231–9. <https://doi.org/10.1016/j.recot.2018.02.007>
7. Ead MS, Duke KK, Jaremko JL, Westover L. Investigation of pelvic symmetry using CAD software. *Med Biol Eng Comput*. 2020;58:75–82. <https://doi.org/10.1007/s11517-019-02068-w>
8. Lima B, Dur O, Chuang J, Chamogeorgakis T, Farrar DJ, Sundareswaran KS, et al. Novel cardiac coordinate modeling system for three-dimensional quantification of inflow cannula malposition of HeartMate II LVADs. *ASAIO J*. 2018;64:154–8. <https://doi.org/10.1097/MAT.0000000000000628>
9. Ramin J, Maureen S, Yuanlong Z, Terry A, Cullen F, Parisa H, et al. Using 3D-Printed Mesh-Like brain cortex with deep structures for planning intracranial EEG electrode placement. *J Digit Imaging*. 2020;33:324–33. <https://doi.org/10.1007/s10278-019-00275-3>
10. Huang F, Chen Y, Li T, Liu H, Mai Q, Fan S. A novel approach for posterior acetabular fractures: surgical technique. *Math Biosci Eng*. 2019;16:7950–62. <https://doi.org/10.3934/mbe.2019400>
11. Choi JW, Ahn JJ, Son K, Huh JB. Three-dimensional evaluation on accuracy of conventional and milled gypsum models and 3D printed photopolymer models. *Materials (Basel)*. 2019;12:3499. <https://doi.org/10.3390/ma12213499>
12. Wang L, Tian D, Liu X, Zhang J, Zhao L, He X, et al. Morphological measurement of supracondylar femur based on digital technology in Chinese han population. *Orthop Surg*. 2019;11:294–303. <https://doi.org/10.1111/os.12443>
13. Yin D, Xin X, Yang R, Shi Y, Shen H. Biomechanical stability of lower cervical spine immediately after discectomy with grafting. *Orthop Surg*. 2011;3:113–8. <https://doi.org/10.1111/j.1757-7861.2011.00132.x>
14. Kulczyk T, Rychlik M, Lorkiewicz-Muszyńska D, Abreu-Głowacka M, Czajka-Jakubowska A, Przysańska A. Computed tomography versus optical scanning: a comparison of different methods of 3D data acquisition for tooth replication. *BioMed Res Int*. 2019;2019:1–7. <https://doi.org/10.1155/2019/4985121>
15. Vandeweghe S, Vervack V, Dierens M, De Bruyn H. Accuracy of digital impressions of multiple dental implants: an in vitro study. *Clin Oral Implants Res*. 2017;28:648–53. <https://doi.org/10.1111/clr.12853>
16. Letournel EJ. *Fractures of the acetabulum*. Berlin: Springer; 1993.
17. Wang C, Liu H, Lin X, Chen J, Li T, Mai Q, et al. A single lateral rectus abdominis approach for the surgical treatment of complicated acetabular fractures: a clinical evaluation study of 59 patients. *Med Sci Monit*. 2018;24:7285–94. <https://doi.org/10.12659/MSM.911009>

18. Chen J, Liu H, Wang C, Lin X, Gu C, Fan S. Internal fixation of acetabular fractures in an older population using the lateral-rectus approach: short-term outcomes of a retrospective study. *J Orthop Surg Res.* 2019;14:4. <https://doi.org/10.1186/s13018-018-1039-z>
19. Wen X, Huang H, Wang C, Dong J, Lin X, Huang F, et al. Comparative biomechanical testing of customized three-dimensional printing acetabular-wing plates for complex acetabular fractures. *Adv Clin Exp Med.* 2020;29:459–68. <https://doi.org/10.17219/acem/116749>
20. Liu Y, Zhan X, Huang F, Wen X, Chen Y, Yang C, et al. The application of lateral-rectus approach on toddlers' unstable pelvic fractures. *BMC Musculoskelet Disord.* 2020;21:147. <https://doi.org/10.1186/s12891-020-3172-1>
21. Wang C, Chen Y, Wang L, Wang D, Gu C, Lin X, et al. Three-dimensional printing of patient-specific plates for the treatment of acetabular fractures involving quadrilateral plate disruption. *BMC Musculoskelet Disord.* 2020;21:451. <https://doi.org/10.1186/s12891-020-03370-7>
22. Boulay C, Tardieu C, Benaïm C, Hecquet J, Marty C, Prat-Pradal D, et al. Three-dimensional study of pelvic asymmetry on anatomical specimens and its clinical perspectives. *J Anat.* 2006;208:21–33. <https://doi.org/10.1111/j.1469-7580.2006.00513.x>
23. Taller S, Srám J, Lukáš R, Endrych L, Džupa V. Fixation of acetabular fractures. A novel method of pre-operative omega plate contouring. *Acta Chir Orthop Traumatol Cech.* 2014;81:212–20. <https://pubmed.ncbi.nlm.nih.gov/24945390/>
24. Osterhoff G, Petersik A, Sprengel K, Pape HC. Symmetry matching of the medial acetabular surface—a quantitative analysis in view of patient-specific implants. *J Orthop Trauma.* 2019;33:e79–83. <https://doi.org/10.1097/BOT.0000000000001373>
25. Ead MS, Westover L, Polege S, McClelland S, Jaremko JL, Duke KK. Virtual reconstruction of unilateral pelvic fractures by using pelvic symmetry. *Int J Comput Assist Radiol Surg.* 2020;15:1267–77. <https://doi.org/10.1007/s11548-020-02140-z>

How to cite this article: Zheng Q, Xu K, Zhan X, Huang F, Wang L, Chen S, et al. Investigation of pelvic symmetry: a systematic analysis using computer aided design software. *Health Care Sci.* 2023;2:36–44. <https://doi.org/10.1002/hcs2.25>